*Colloids and Surfaces A: Physicochemical and Engineering Aspects*, 80 (1993) 69–75
0927-7757/93/$06.00 



# Structure and magnetic properties of nanoparticles of barium ferrite synthesized using microemulsion processing

Vinod Pillai, Promod Kumar, Manu S. Multani[1], Dinesh O. Shah*
*Center for Surface Science and Engineering, Departments of Chemical Engineering & Anesthesiology, University of Florida, Gainesville, FL 32611, USA*

(Received 28 September 1992; accepted 8 April 1993)

**Abstract**

Nanoparticles of barium ferrite ($BaFe_{12}O_{19}$) were synthesized using a novel method called microemulsion processing. In this process, the aqueous cores (typically 5–25 nm in size) of water–cetyltrimethylammonium bromide–*n*-butanol–octane microemulsions were used as constrained microreactors for the co-precipitation of precursor carbonates (typically 5–15 nm in size). The carbonates thus formed were separated, dried and calcined to form nanoparticles (less than 100 nm) of barium ferrite. The particle size and size distribution were determined by transmission electron microscopy. Phase analysis of the final product by X-ray diffraction confirmed the formation of hexagonal barium ferrite. The powder was further characterized by the measurement of magnetic properties such as coercive field $H_c$, saturation magnetization $M_s$, remanent magnetization $M_r$ and loop squareness $S_r$.

*Key words:* Barium ferrite; Coercivity; Magnetization; Microemulsion; Microemulsion processing; Nanoparticles

## Introduction

Synthesis of particles with nanometer size dimensions is of increasing scientific and technical interest. Materials with single-phase nanoparticles in the size range 10–100 Å exhibit novel electronic, optical, magnetic and chemical properties owing to their extremely small dimensions [1]. It is, however, difficult to obtain ultrafine and monodispersed nanoparticles by classical methods. In this respect, the aqueous cores of water-in-oil microemulsions have been shown to be ideal reaction media for this purpose [2].

[1]Present address: Solid State Physics Division, Tata Institute of Fundamental Research, Bombay, India.
*Corresponding author.

### *Microemulsions as microreactors*

A microemulsion is generally defined as a thermodynamically stable isotropic dispersion of two immiscible liquids consisting of microdomains of one or both liquids stabilized by an interfacial film of surface-active molecules [3]. In water-in-oil microemulsions, the aqueous phase is dispersed as nano-size droplets (typically 5–25 nm in size) surrounded by a monolayer of surfactant and co-surfactant molecules in the continuous hydrocarbon phase. If a water-soluble metal salt is incorporated in the aqueous phase of the microemulsion, it will reside within the aqueous droplets surrounded by oil (continuous phase). These aqueous droplets continuously collide, coalesce and decoalesce, resulting in a continuous exchange of solute content [4,5]. Conceptually, if two reactants A and B are dissolved in the aqueous cores of two

identical water-in-oil microemulsions, upon mixing they will form an AB complex and precipitate. The chemical reaction between the two reactants A and B is controlled by the rate of coalescence of droplets and the interdroplet exchange [5,6].

Microemulsions have been used as microreactors to produce ultrafine particles since Boutonnet et al. [2] first obtained ultrafine monodispersed metal particles of platinum, palladium, rhodium and iridium by reducing corresponding salts in the aqueous droplets of water-in-oil microemulsions with hydrazine or hydrogen gas. Water-in-oil microemulsions have also been used to synthesize nanoparticles of metal borides [7], silver halides [8,9], $BaCO_3$ [10] and oxalate precursors for $YBa_2Cu_3O_{7-x}$ superconductors [11]. In this paper, we report the synthesis of nanoparticles of barium iron carbonate in water-in-oil microemulsions for the preparation of ultrafine barium ferrite particles.

*Barium ferrite*

Barium ferrite ($BaFe_{12}O_{19}$) has traditionally been used in permanent magnets because of its high intrinsic coercivity and fairly large crystal anisotropy [12]. However, in the past decade it has emerged as an important magnetic medium for high density perpendicular recording [13]. This has led to an increasing demand for the preparation of ultrafine magnetic oxides of uniform size which can be used for computer data storage, audio and video recording, magnetic fluids and fabrication of certain microwave devices [14]. Such technological applications require materials with strictly controlled homogeneity, particle size and shape, and magnetic characteristics.

The classical ceramic method for the preparation of barium ferrite consists of firing mixtures of iron oxide and barium carbonate at high temperatures (about 1200°C) [15,16]. Furthermore, the ferrite must then be ground to reduce the particle size from multi to single domain. This generally yields mixtures which are non-homogeneous on a microscopic scale. Milling introduces lattice strains in the material, whereas high reaction temperatures induce sintering and coagulation of particles, both of which can be damaging if specific properties like uniform and reduced particle sizes, and high coercivities are required in the final product [17,18].

In order to achieve a homogeneity of ions at the atomic level, and to overcome the effects of milling, various techniques such as chemical coprecipitation [19–21], glass crystallization [13,22], the organometallic precursor method [23,24], aerosol synthesis [25,26] and colloidal synthesis [27] have been developed to prepare ultrafine barium ferrite. We have used the aqueous cores of water-in-oil microemulsions as reaction media to produce uniform-sized microhomogeneous nanoparticles of carbonate precursors for the synthesis of ultrafine barium ferrite.

## Experimental

*Materials*

Barium nitrate and ferric nitrate (more than 99.99% pure) were purchased from Aldrich. Ammonium carbonate (HPLC grade), cetyltrimethylammonium bromide (CTAB) (technical grade), and *n*-butanol, methanol and chloroform (all HPLC grade) were purchased from Fisher. Octane (more than 99% pure) was purchased from Sigma. All reagents were used without further purification. Water was deionized and distilled before use.

*Methods*

We selected a microemulsion system with CTAB as the surfactant, *n*-butanol as the cosurfactant, *n*-octane as the continuous oil phase, and a salt solution as the dispersed aqueous phase (see Table 1 for the compositions). This system solubilizes a relatively large volume of aqueous phase in well-defined nano-size droplets of stable single-phase water-in-oil microemulsions [11].

Microemulsions were prepared by solubilizing different salt solutions into CTAB–*n*-butanol–

Table 1
Composition of the microemulsion systems used for the synthesis reactions

| | Microemulsion I | Microemulsion II | Weight fraction |
|---|---|---|---|
| Aqueous phase | 0.011 M $Ba(NO_3)_2$ +0.12 M $Fe(NO_3)_3$ | 0.19 M $(NH_4)_2CO_3$ | 0.34 |
| Surfactant | CTAB | CTAB | 0.12 |
| Cosurfactant | *n*-Butanol | *n*-Butanol | 0.10 |
| Oil phase | *n*-Octane | *n*-Octane | 0.44 |

*n*-octane solutions. We took two microemulsions (microemulsion I and microemulsion II) with identical compositions (see Table 1) but different aqueous phases. The aqueous phase in microemulsion I was a mixture of barium nitrate and ferric nitrate solutions in the molar ratio of 1.1 : 12. Even though, according to stoichiometry, a ratio of 1 : 12 should be sufficient, an excess of barium nitrate was used because it is necessary for the precipitation of $Ba^{2+}$ and $Fe^{3+}$ ions in the ratio of 1 : 12 as barium carbonate is partially soluble in water. The aqueous phase in microemulsion II was the precipitating agent, ammonium carbonate, taken in the stoichiometric quantity required for complete precipitation of the cations. These two microemulsions were then mixed under constant stirring. Owing to the frequent collisions of the aqueous cores of water-in-oil microemulsions [4,5], the reacting species in microemulsions I and II come in contact with each other. This leads to the precipitation of barium iron carbonate within the nano-size aqueous droplets of the microemulsion. Since the two microemulsions (I and II) are of identical compositions, differing only in the nature of the aqueous phase, the microemulsion does not become destabilized upon mixing. The aqueous droplets act as constrained nano-size reactors for the precipitation reaction, as the surfactant monolayer provides a barrier restricting the growth of the carbonate particles. This surfactant monolayer also hinders coagulation of particles. A schematic representation of this process is shown in Fig. 1.

The barium iron carbonate precipitate was separated in a Sorvall RC-5B Superspeed Centrifuge at 5000 rev $min^{-1}$ for 10 min. The precipitate was

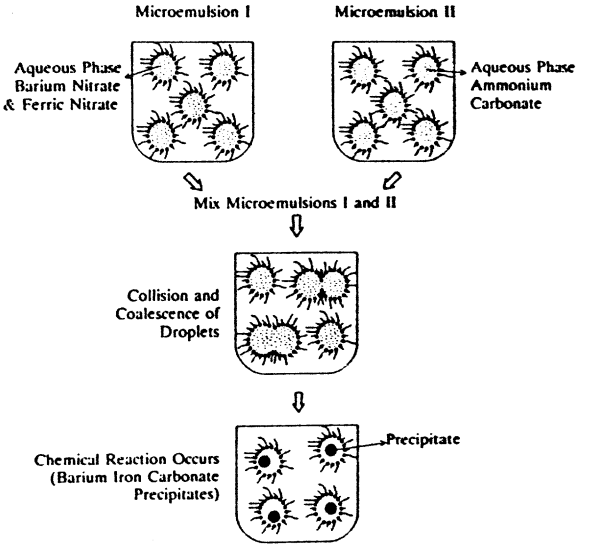


Fig. 1. Schematic representation of the reaction in microemulsions.

then washed in a 1 : 1 mixture of methanol and chloroform, followed by pure methanol to remove any oil and surfactant from the particles. The precipitate was then dried at 100°C. Sintering of particles is not expected at this temperature.

Thermogravimetric analysis (TGA) was done on the dried powder in air with a heating rate of 5°C $min^{-1}$ on a DuPont 900 Series TGA/DTA instrument. Differential thermal analysis (DTA) was done on the dried powder in air with a heating rate of 10°C $min^{-1}$. Based on the results of these analyses (discussed in the next section), the dried precipitate was heated (calcined) at 950°C for 12 h to ensure complete conversion of the carbonates into the hexaferrite ($BaFe_{12}O_{19}$).

Transmission electron microscopy (TEM) was

used to study the size and size distribution of the precursor particles (carbonates) as well as the calcined particles. In order to study the precursors, the washed precipitate was ultrasonically dispersed in methanol prior to depositing it onto a carbon-coated TEM grid. TEM of the final product was done by ultrasonically dispersing the calcined powder in methanol prior to depositing it onto a carbon-coated TEM grid. A JEOL 200CX transmission electron microscope was used for these studies.

Phase analysis of the calcined powder was done by powder X-ray diffraction (XRD) on a Phillips PW1700 powder diffractometer at room temperature using Cu Kα radiation at 40 kV and 20 mA.

Magnetization (MH loop) measurements were done on an unoriented random assembly of particles at room temperature on a vibrating sample magnetometer (VSM) (LDJ 9600) with a maximum applied field of 15 kOe. The sample was prepared by hand pressing the calcined powder into a cylindrical pellet. No further heat treatment was done on the pellet.

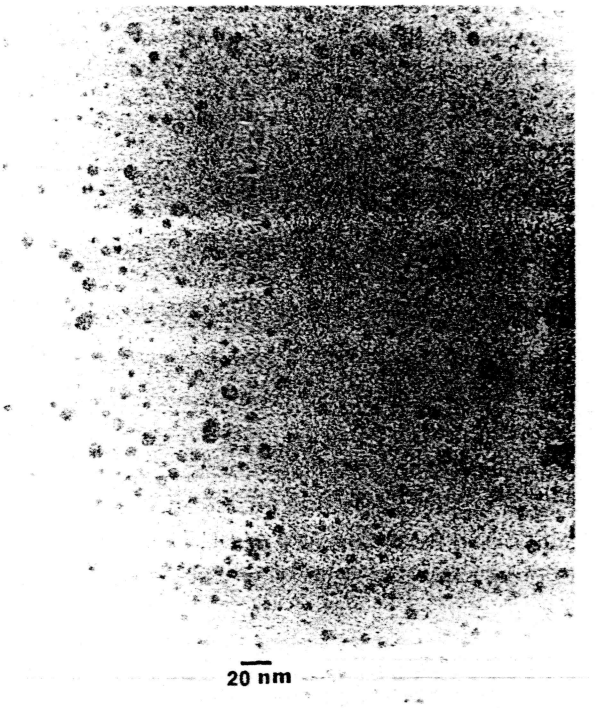


Fig. 2. Transmission electron micrograph of precursor carbonates.

## Results and discussion

The transmission electron micrograph of the precursor carbonates (Fig. 2) shows that the precursor particles formed within the aqueous droplets of the microemulsion are fairly monodispersed with a size range of 5–15 nm. In contrast, however, the transmission electron micrograph of the calcined powder (Fig. 3) shows that these particles are in the size range 50–100 nm, implying that growth of particles has taken place during calcination.

The TGA curve (Fig. 4) shows three distinct weight loss steps. These steps are associated with the vaporization of water and organic moieties, and the conversion of ferric carbonate and barium carbonate into their respective oxides. It can also be seen from this graph that there is no weight change above 900°C, indicating the existence of only the oxide above this temperature. The DTA curve (Fig. 5) shows an exothermic peak associated with the sharp weight loss in the TGA curve. A magnified view of this curve (see inset of Fig. 5) shows that a small endotherm exists around 923°C, implying that phase transformation to the hexaferrite occurs around this temperature. Therefore calcination of the precursors was done at 950°C to ensure complete phase transformation.

The XRD pattern for the calcined powder (Fig. 6) shows all the characteristic peaks for barium ferrite, marked by their indices. No other phases are detectable. This confirms the complete conversion of the precursor carbonates into the hexagonal ferrite $BaFe_{12}O_{19}$.

The room temperature magnetization curve for the calcined powder, obtained on the VSM, is shown in Fig. 7. The magnetic property measurements yielded an intrinsic coercivity $H_c$ of 5397 Oe and a saturation magnetization $M_s$ of 61.2 emu $g^{-1}$ (see Table 2 for a complete list of the magnetic properties measured). This high value of coercivity indicates that the barium ferrite particles formed by microemulsion processing are essentially single


Fig. 3. Transmission electron micrograph of microemulsion-derived barium ferrite particles.

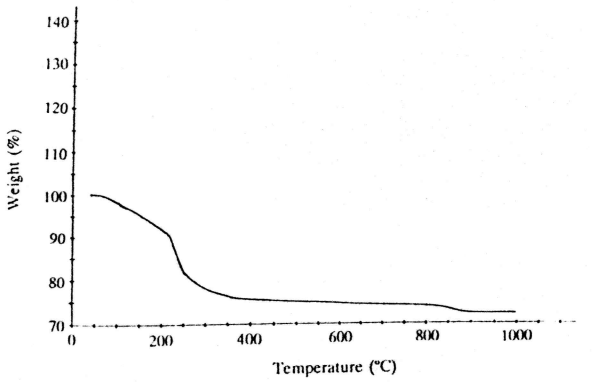


Fig. 4. Thermogravimetric analysis of precursor carbonates.

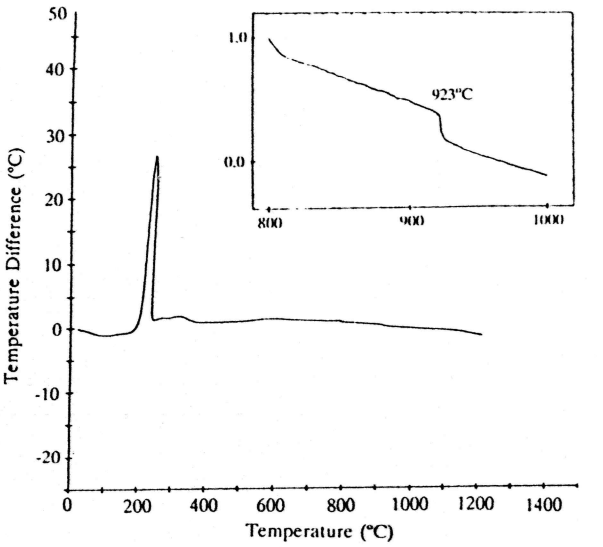


Fig. 5. Differential thermal analysis of precursor carbonates.

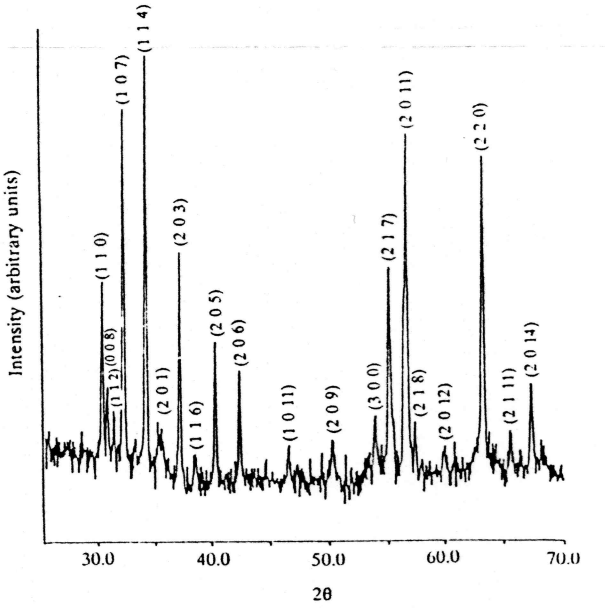


Fig. 6. X-ray diffraction pattern of microemulsion-derived barium ferrite particles using Cu Kα radiation.

domain. This observation is also confirmed by the fact that the particles formed by us are in the size range 50–100 nm. Haneda and Morrish [28] have shown that using the theory of Kittel [29], the critical domain size for barium ferrite particles is about 1 μm. Further, direct observation of the domain structure of barium ferrite particles at room temperature by Goto et al. [30] confirms that the domain critical size is indeed in the region of 1 μm.

However, the value of intrinsic coercivity $H_c$

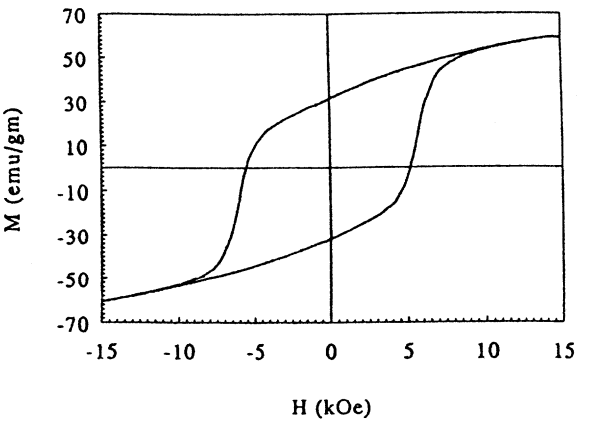


Fig. 7. Room temperature magnetization curve for barium ferrite particles on a VSM.

Table 2
Magnetic properties of microemulsion-derived barium ferrite

| | |
|---|---|
| Saturation magnetization $M_s$ | 61.2 emu $g^{-1}$ |
| Intrinsic coercivity $H_c$ | 5397 Oe |
| Remanent magnetization $M_r$ | 33.3 emu $g^{-1}$ |
| Squareness ratio $S_r$ | 0.54 |

obtained for our sample is lower than that theoretically calculated ($H_c \approx 6700$ Oe) [31] using the model proposed by Stoner and Wohlfarth [32] for an unoriented assembly of uniaxial single-domain particles in which magnetization reversal has occurred through uniform rotation. The value of the saturation magnetization $M_s$ is also lower than the saturation magnetization for single crystals of $BaFe_{12}O_{19}$ ($M_s$ of 72 emu $g^{-1}$ as reported by Shirk and Buessem [33]). Haneda et al. [20] have reported that reverse-domain nucleation greatly influences the intrinsic coercivity of precipitated powders. Reverse-domain nucleation may arise, even for stress-free chemically precipitated barium ferrite, at the edge of the particles. This may explain the discrepancy between experimental and theoretically calculated values of $H_c$ and $M_s$ for barium ferrite formed by microemulsion processing. Another reason may be poor crystallization of $BaFe_{12}O_{19}$ particles, leading to amorphous impurities undetectable by XRD.

## Conclusions

In this paper we have presented a new process for the synthesis of ultrafine nanoparticles of barium ferrite. Aqueous droplets of water-in-oil microemulsions have been used as nano-size reactors to precipitate precursor carbonates of barium and ferric salts. These precursors have been calcined to produce ultrafine high coercivity barium ferrite, as confirmed by X-ray diffraction and magnetization measurements. The elimination of all amorphous impurities by further optimization of the process should produce phase-pure particles with ideal single-domain behavior with coercivity and saturation magnetization close to theoretically predicted values. These phase-pure single-domain particles can then be doped by cobalt and titanium to reduce the coercivity and large anisotropy to make these particles suitable for high density perpendicular recording [13].

## Acknowledgments

The authors wish to thank the National Science Foundation (Grant no. NSF-CTS 8922574) for supporting this research.

## References

1 R.P. Andres, R.S. Averback, W.L. Brown, L.E. Brus, W.A. Goddard III, A. Kaldor, S.G. Louie, M. Moskovits, P.S. Peercy, S.J. Riley, R.W. Seigel, F. Spaepen and Y. Wang, J. Mater. Res., 4 (1989) 704.
2 M. Boutonnet, J. Kizling, P. Stenius and G. Maire, Colloids Surfaces, 5 (1982) 209.
3 R. Leung, M.J. Hou, C. Manohar, D.O. Shah and P.W. Chun, in D.O. Shah (Ed.), Macro- and Microemulsions, American Chemical Society, Washington, DC, 1981, p. 325.
4 H.F. Eicke, J.C.W. Shepherd and A. Steinemann, J. Colloid Interface Sci., 56 (1976) 168.
5 P.D.I. Fletcher, A.M. Howe and B.H. Robinson, J. Chem. Soc., Faraday Trans. 1, 83 (1987) 985.
6 J.H. Fendler, Chem. Rev., 87 (1987) 877.
7 N. Lumfimpadio, J.B. Nagy and E.G. Derouane, in K. Mittal and B. Lindman (Eds.), Surfactants in Solution, Vol. 3, Plenum, New York, 1986, p. 483.
8 M.J. Hou and D.O. Shah, in Y.A. Attia, B.M. Moudgil and S. Chander (Eds.), Interfacial Phenomena in Biotechnology and Materials Processing, Elsevier, Amsterdam, 1988, p. 443.

9 C.H. Chew, L.M. Gan and D.O. Shah, J. Dispersion Sci. Technol., 11 (1990) 593.
10 K. Kon-no, M. Koide and A. Kitahara, J. Chem. Soc. Jpn., 6 (1984) 815.
11 P. Ayyub, A.N. Maitra and D.O. Shah, Physica C, 168 (1990) 571.
12 B.D. Cullity, Introduction to Magnetic Materials, Addison-Wesley, Reading, MA, 1972, p. 575.
13 O. Kubo, T. Ido and H. Yokoyama, IEEE Trans. Magn., 18 (1982) 1122.
14 F. Okada, in F.F.Y. Wang (Ed.), Proc. 4th Int. Conf. on Ferrites, Part II, The American Ceramic Society, Inc., Columbus, OH, 1984, Vol. 16, p. 1.
15 H. Kojima, in E.P. Wohlfarth (Ed.), Ferromagnetic Materials, Vol. 3, North-Holland, Amsterdam, 1982, p. 305.
16 G.C. Bye and C.R. Howard, J. Appl. Chem. Biotechnol., 21 (1971) 319.
17 K. Haneda and H. Kojima, J. Am. Ceram. Soc., 57 (1974) 68.
18 M. Paulus, Preparative Methods in Solid State Chemistry, Academic Press, New York, 1972, p. 488.
19 C.D. Mee and J.C. Jeschke, J. Appl. Phys., 34 (1963) 1271.
20 K. Haneda, C. Miyakama and H. Kojima, J. Am. Ceram. Soc., 57 (1974) 354.
21 W. Roos, J. Am. Ceram. Soc., 63 (1980) 601.
22 B.T. Shirk and W.R. Buessem, J. Am. Ceram. Soc., 53 (1970) 192.
23 F. Licci and T. Besagni, IEEE Trans. Magn., 20 (1984) 1639.
24 M. Vallet, P. Rodriguez, X. Obradors, A. Isalgue, J. Rodriguez and M. Pernet, J. Phys. (Paris), 46 (1985) C6-335.
25 Z.X. Tang, S. Nafis, C.M. Sorensen, G.C. Hadjipanayis and K.J. Klahunda, IEEE Trans. Magn., 25 (1989) 4236.
26 W.A. Kaczmarek, B.W. Ninham and A. Calka, J. Appl. Phys., 70 (1991) 5909.
27 E. Matijevic, J. Colloid Interface Sci., 117 (1987) 593.
28 K. Haneda and A.H. Morrish, IEEE Trans. Magn., 25 (1989) 2597.
29 C. Kittel, Rev. Mod. Phys., 40 (1969) 1294.
30 K. Goto, M. Ito and T. Sakurai, Jpn. J. Appl. Phys., 19 (1980) 541.
31 K. Haneda and H. Kojima, J. Appl. Phys., 44 (1973) 3760.
32 E.C. Stoner and E.W. Wohlfarth, Philos. Trans. R. Soc. London, Ser. A, 240 (1948) 599.
33 B.T. Shirk and W.R. Buessem, J. Appl. Phys., 40 (1969) 1294.